# Enricofrancoite, $KNaCaSi_4O_{10}$, a new Ca-K-Na silicate from Somma-Vesuvius volcano, southern Italy

Giuseppina Balassone[1,2,3], Taras L. Panikorovskii[4,5*], Annamaria Pellino[1], Ayya V. Bazai[4], Vladimir N. Bocharov[6], Olga F. Goychuk[4], Evgenia Yu. Avdontseva[5], Victor N. Yakovenchuk[5], Sergey V. Krivovichev[5], Carmela Petti[7], Piergiulio Cappelletti[1,2,7], Nicola Mondillo[1], Anna Moliterni[8], Angela Altomare[8], Francesco Izzo[1,2]

[1]Department of Earth Science, Environment and Resources (DiSTAR), University of Naples Federico II, Via Cintia, 26, Naples I-80126, Italy

[2]Center for Research on Archaeometry and Conservation Science (CRACS), University of Naples Federico II, Via Cintia, 26, Naples I-80126, University of Sannio, Via dei Mulini 73, Benevento I-82100, Italy

[3]National Institute of Geophysics and Volcanology (INGV), Vesuvius Observatory, Via Diocleziano I-80124 Naples, Italy

[4]Kola Science Centre, Russian Academy of Sciences, 14 Fersman Street, Apatity 184200, Russia

[5]Department of Crystallography, St. Petersburg State University, 7–9 Universitetskaya Naberezhnaya, St. Petersburg 199034, Russia

[6]Geo Environmental Centre "Geomodel", Saint-Petersburg State University, 1 Ul'yanovskay Str., St. Petersburg 198504, Russia

[7]Centro Museale "Centro Musei delle Scienze Naturali e Fisiche", University of Naples Federico II, Via Mezzocannone 8, 80134 Napoli, Italy

[8]Istituto di Cristallografia, CNR, Via Amendola 122/O, 70126 Bari, Italy



This is a 'preproof' accepted article for Mineralogical Magazine. This version may be subject to change during the production process.
DOI: 10.1180/mgm.2024.9

*Author for correspondence: Taras L. Panikorovskii, t.panikorovskii@ksc.ru

Running title: Enricofrancoite, a new Ca-Na-K silicate

**Abstract**

Enricofrancoite (IMA 2023-002), ideally $KNaCaSi_4O_{10}$, is a new litidionite-group member found as the product of high-temperature alteration of hosting silicates with the enrichment by Cu-bearing fluids at the rock-fumaroles interface related to the 1872 eruption of Somma-Vesuvius volcano, southern Italy. It occurs as euhedral and platy crystals or crusts together with litidionite, tridymite, wollastonite and Al- and Fe-bearing diopside, kamenevite, perovskite, rutile, Ti-rich magnetite and colorless Si-glass. Single crystals of enricofrancoite are transparent colorless or light blue with a vitreous lustre. Mohs hardness is 5.5. $D_{meas}$ is 2.63(3) g/cm$^3$ and $D_{calc}$ is 2.63 g/cm$^3$. The mineral is optically biaxial (−), α = 1.542(5), β = 1.567(5),γ = 1.575(5); $2V_{(meas)}$ = 60(2)° and $2V_{calc}$ = 58°. The mean chemical composition (wt.%, electron-microprobe data) is: $SiO_2$ 64.81, $Al_2O_3$ 0.03, $TiO_2$ 0.08, FeO 0.07, MgO 1.71, CaO 10.64, CuO 2.22, $Na_2O$ 8.56, $K_2O$ 11.41, total 99.94. The empirical formula based on 10 O *apfu* is: $K_{0.90}Na_{1.03}(Ca_{0.71}Mg_{0.16}Cu_{0.10})_{\Sigma=0.97}Si_{4.02}O_{10}$. The Raman spectrum contains bands at 133, 248, 265, 290, 335, 400, 438, 510, 600, 690, 1120 cm$^{-1}$ and the wavenumbers of the IR absorption bands are: 424, 470, 492, 530, 600, 630, 690, 750, 788, 970, 1040, 1160 cm$^{-1}$. The eight strongest lines of the powder X-ray diffraction pattern are (*I*-*d*(Å)-*hkl*): 42-6.75-01-1, 20-3.65-11-2, 100-3.370-02-2, 52-3.210-102, 18-3.051-111, 25-3.033-2-1-2, 22-2.834-02-3, 72-2.411-03-2. Enricofrancoite is triclinic, space group *P*-1, unit-cell parameters refined from the single-crystal data are $a$ = 7.0155(4) Å, $b$ = 8.0721(4) Å, $c$ = 10.0275(4) Å, α = 104.420(4)°, β = 99.764(4)°, γ = 115.126(5)°, V = 472.74(5) Å$^3$. The crystal structure has been refined from single-crystal X-ray diffraction data to $R_1$ = 0.035 on the basis of 2078 independent reflections with $F_o > 4\sigma(F_o)$. Enricofrancoite is an $H_2O$-free analogue of calcinaksite with 5-coordinated $Ca^{2+}$ at the *M* site.

**Keywords:** new mineral, enricofrancoite, litidionite group, crystal structure, Somma-Vesuvius, Italy

## Introduction





https://doi.org/10.1180/mgm.2024.9 Published online by Cambridge University Press

Enricofrancoite is a new mineral found in rare litidionite-bearing samples of the Somma-Vesuvius volcano, southern Italy (40°49'17"N, 14°25'35"E). The specimen of enricofrancoite in this study was collected, together with other samples of the same type, in the Royal Mineralogical Museum of Naples (henceforth RMMN, nowadays part of "Centro Musei delle Scienze Naturali e Fisiche") of the University Federico II (Italy) in 1873. In June of that year, a mineral collector found small lapilli covered by deep-blue crusts with a peculiar glassy-to enameled-like appearance, related to the 1872 AD, at the Vesuvius crater and brought them to Arcangelo Scacchi, director of the Museum at that time.

Enricofrancoite is named in honor of Enrico Franco (1927–2009), professor of Mineralogy at the University of Naples Federico II, Italy. Prof. Franco was the author of many papers regarding mineralogy and made a significant contribution to the field of mineralogy of Somma-Vesuvius volcano, where he also discovered the panunzite (the natural counterpart of tetrakalsilite) and the chabazite-K (de Gennaro and Franco, 1974; Merlino *et al.*, 1985; Franco and de Gennaro, 1988).

The new mineral and its name (symbol Enf) were approved by the Commission of New Minerals, Nomenclature and Classification of the International Mineralogical Association (IMA 2023-002) (Balassone et al., 2023). The holotype specimen is deposited in the systematic collection of the Vesuvian Collection of the RMMN, with the catalogue number 17926 E6457.

## Occurrence

The specimen with the new mineral (Fig. 1) belongs to a set of samples from Vesuvius volcano (40°49'17"N, 14°25'35"E), which contains the rare litidionite-bearing assemblage (Pozas *et al.*, 1975; Balassone *et al.*, 2019, 2022). The new mineral occurs in a complex paragenesis composed of litidionite, tridymite, wollastonite and Al- and Fe-bearing diopside, kamenevite, perovskite, rutile, Ti-rich magnetite, and an amorphous phase, in deep blue to white crusts covering metamorphosed lapilli





https://doi.org/10.1180/mgm.2024.9 Published online by Cambridge University Press

related to the 1872 eruption. Various trace non-silicates are also recorded, and further minor to trace phases will very likely be identified in this mineral assemblage from Vesuvius in our ongoing research on new sample sets.

Ti- and Pb-bearing litidionite are also reported (Balassone *et al.*, 2022); moreover, in the white crust, the Ca-Na-K-bearing silicate, in the first instance was identified as calcinaksite by the above authors. This mineral association is typical of high-temperature alteration processes at the rock-fumaroles interface (Pozas *et al.*, 1975; Balassone *et al.*, 2019, 2022) as a product of very localized high-temperature (exhalation-related) alteration processes of hosting silicates and the introduction of other chemical components by fluids (e.g., $Cu^{2+}$). This peculiar assemblage, like that observed for the Eifel region calcinaksite-bearing rocks (Aksenov et al., 2014; Chukanov et al., 2015), can likely occur at a temperature of > 600 °C. Further chemical investigations mainly on the white assemblage revealed a significant mineral component corresponding to an anhydrous analogue of calcinaksite, which was then named enricofrancoite. In the observed mineral assemblage, there are four different types of litidionite-group minerals which crystallize in the following order: euhedral and platy crystals of litidionite or Ca-bearing litidionite up to enricofrancoite → altered zones around diopside crystals consisting of litidionite or fine-grained litidionite → coarse-grained enricofrancoite crystals in the litidionite matrix → marginal zones of lapilli represented by Ti-bearing non-stoichiometric litidionite (Balassone *et al.*, 2022). Based on our new evidence, most of calcinaksite previously indicated should be in fact enricofrancoite.

**Physical and optical properties**

The morphology of the minerals was studied using of Jeol JSM5310 scanning electron microscope with an Oxford EDS equipped with an INCA X-stream pulse processor and the 4.08 version Inca software (Department of Earth Science, Environment and Resources, DiSTAR, University of Naples Federico II Italy). Enricofrancoite forms platy crystals in fine-grained aggregations (Fig. 2), rarely to





https://doi.org/10.1180/mgm.2024.9 Published online by Cambridge University Press

1 mm in length. Mineral forms colourless, translucent, non-fluorescent individual crystals, with a white streak and vitreous lustre. The mineral is brittle, with a stepped fracture, a good {001} cleavage. The calculated density is 2.63 g/cm$^3$, from single-crystal X-ray diffraction (SC-XRD) data, as the measured density by flotation in Clerici solution, i.e. 2.63(3) g/cm$^3$. The compatibility index is –0.049, good based on empirical formula and measured density. Mohs hardness is assumed to be 5.5. The new mineral is transparent and optically biaxial (−), the refractive indices were measured at white light: $\alpha = 1.542(5)$, $\beta = 1.567(5)$ and $\gamma = 1.575(5)$. The $2V_{(meas)} = 60(2)°$ and $2V_{calc} = 58°$. The 2V was measured using the formula $\sin V = KD/\beta$, where D is the distance in conoscopy between the vertices of the hyperbola branches at their maximum divergence (measured with an eyepiece equipped with a micrometer ruler); β is the refractive index; K is a coefficient depending on the optical system of the microscope, which was calculated using a standard with a known value of 2V (phlogopite - 16°). The dispersion is weak (r < v), and it is non-pleochroic. The optical orientation is $Z \approx b$, $Y \wedge c = 49°$ and $Z \wedge a \approx 90°$.

**Chemical composition**

Chemical composition was determined with the Cameca MS-46 electron microprobe operating in a wavelength-dispersive mode (WDS) at 20 kV and 20–30 nA and a spot size of 10 μm at the Geological Institute of the Kola Science Center, Apatity. The following standards were used: lorenzenite (Na, Ti), pyrope (Mg, Al), diopside (Si, Ca), wadeite (K), hematite (Fe), metallic niobium (Nb), metallic copper (Cu), wulfenite (Pb) and atacamite (Cl). The mean analytical results of 3 selected crystals (five spots for each crystal, with a total of 15 analyses) are given in Table 1. Cation contents were calculated with the MINAL program of D. Dolivo-Dobrovolsky (Dolivo-Dobrovolsky, 2016). $H_2O$ was not analyzed because of the absence of bands corresponding to the O-H vibrations in the Raman and FTIR spectra.

The empirical formula calculated on the basis of O=10 *apfu* is





https://doi.org/10.1180/mgm.2024.9 Published online by Cambridge University Press

$K_{0.90}Na_{1.03}(Ca_{0.71}Mg_{0.16}Cu_{0.10})_{\Sigma=0.97}Si_{4.02}O_{10}$. The analyses of enricofrancoite crystals reveal a substitution between $Ca^{2+}$, $Mg^{2+}$ and $Cu^{2+}$ nearly equal to 0.1 *apfu*. It seems that the Cu – Ca substitution forms a continuous series between litidionite and enricofrancoite. The amount of Mg is also variable and is possible occurrence of Mg-analogue of enricofrancoite in the same mineral association. According to our previous data, the $Ti^{4+}$ (analysis No 2 in Table 1) is also incorporated into the *M* site together with the Mg, Cu and Fe. This substitution also may include K/vacancy variation in composition (Balassone *et al.*, 2022). The simplified formula is KNa(Ca,Mg,Cu)$Si_4O_{10}$.The ideal formula is $KNaCaSi_4O_{10}$, which requires $K_2O$ 12.58%, CaO 14.97%, $Na_2O$ 8.28%, $SiO_2$ 64.18%.

**Crystal structure solution and refinement**

The grain selected for optical study was also used for single-crystal X-ray diffraction. The studied crystal was mounted on an Oxford Diffraction Xcalibur Eos diffractometer equipped with a CCD area detector using Mo*K*α radiation (0.71073 Å) at the X-ray Diffraction Resource Centre of St. Petersburg State University. More than a half sphere of the diffraction sphere was collected (scanning step 1°, exposure time 75 s). The data were integrated and corrected by means of the CrysAlisPro program package, which was also used to apply an empirical absorption correction using spherical harmonics, as implemented in the SCALE3 ABSPACK scaling algorithm (Agilent Technologies, 2014). The crystal structure was drawn using the VESTA 3 program (Momma and Izumi, 2011). The distortion indexes for polyhedra were calculated according to the formula proposed by Baur, (1974).

Since the calcinaksite and enricofrancoite are chemically very close, the structure of enricofrancoite was refined using the initial calcinaksite model (Chukanov *et al.*, 2015) without O11 (Ow) site to $R_1 = 0.035$ for 2078 independent reflections with $F_o > 4\sigma(F_o)$ using Olex2 (Dolomanov *et al.*, 2009) with the SHELXL (Sheldrick, 2015). Initially the *M* site refined with full occupancy by Ca atoms only, but the Bond-valence analysis demonstrated overestimated sum (2.45 *v.u.*), which





https://doi.org/10.1180/mgm.2024.9 Published online by Cambridge University Press

probably connected with admixtures of Mg and Cu with smaller ionic radii than Ca. According to the EMPA data the composition of *M* site should be $(Ca_{0.71}Mg_{0.16}Cu_{0.10})_{0.97}$. At the final stage of refinement, the *M*1 site occupancy were fixed with $(Ca_{0.71}Mg_{0.19}Cu_{0.10})_{1.00}$. The $R_1$ factor slightly improved from 0.0353 in model with $Ca_{1.00}$ occupancy to 0.0348 for the last data with mixed occupancy. The SC-XRD data are deposited in the CCDC under the entry No. 2292985. Crystal data, data collection information and structure refinement details are given in Table 2. Atom coordinates, anisotropic atomic displacement parameters, and selected interatomic distances are presented in Tables 3, 4 and 5, respectively.

**Powder X-ray diffraction**

Powder X-ray diffraction (PXRD) data were collected using a Seifert-GE diffractometer ID 3003; the intensity profiles were collected in the 2θ range of 3-80°, using Ni-filtered CuKα radiation at 40 kV and 30 mA, with a step size 0.02°, at a scanning time of 10 s/step. The diffraction patterns were processed using the RayfleX software package. Measurements on the mineral assemblages were also carried out by an automated Rigaku RINT2500 rotating anode laboratory diffractometer (50 kV, 200 mA) equipped with the silicon strip Rigaku D/teX Ultra detector, and an asymmetric Johansson Ge (111) crystal (to select the monochromatic CuKα1 radiation λ= 1.54056 Å) and using a glass capillary (0.5 mm diameter). The intensity values $I_{calc}$ for enricofrancoite were calculated by VESTA 3 program from single-crystal X-ray data. They are given in Table 6 with the corresponding intensities $I_{meas}$ measured from the PXRD data using the software Analyze RayfleX GE Insp. Techn. ver. 2.3.3.7, in addition to the calculated ($d_{calc}$) and measured ($d_{meas}$) interplanar distance values and Miller indices (*hkl*). The unit-cell parameters were calculated using UNITCELL software (Holland and Redfern, 1997). The unit-cell parameters refined from the PXRD data are as follows: $a$ = 7.071(2) Å, $b$ = 8.089(2) Å, $c$ = 9.933(2) Å, α = 104.35(2)°, β = 99.51(2)°, γ = 115.28(1)°, V = 473.3(1) Å$^3$, space group *P*-1 (#2) and $Z$ = 2, which are in good agreement with the single-crystal X-ray diffraction data





https://doi.org/10.1180/mgm.2024.9 Published online by Cambridge University Press

(Table 2).

**Structure description**

The crystal structure of enricofrancoite is chemically close to that of litidionite one and consists of complex heteropolyhedral framework (Fig. 3a). The main feature of litidionite-related crystal structures is one-dimensional infinite anionic tubes $[Si_8O_{20}]^{8-}{}_\infty$ running along [100] (Fig. 3b). Enricofrancoite should be classified as loop-branched dreier double chain {***lB***, $2^1{}_\infty$} [$^3Si_8O_{20}$] in accordance with the Liebau classification (Liebau, 1985) or $^3T_8$ silicate tube-containing mineral according to structure hierarchy for silicate minerals (Day and Hawthorne, 2020). Tubes with the same topology are also observed in the agrellite structure, although they have differences. A $^3T_8$ ribbon is also present in the titanosilicate narsarsukite, which has a different structure and crystal system. Each tube consists of four symmetrically independent Si tetrahedra with Si−O bond distances in the range 1.567-1.634 Å. The mean bond lengths for the <Si1−O>, <Si2−O>, <Si3−O> and <Si4−O> tetrahedra are 1.614, 1.599, 1.605, 1.617 Å, respectively, in agreement with the full occupancy of all tetrahedral sites by Si atoms.

Silicate tubes are connected to each other through the $[Ca_2O_8]^{12-}$ dimers, which form layers along *ab* plane (Fig. 3c) and build a three-dimensional framework (Fig. 3d) (Golovachev *et al.*, 1970; Kornev *et al.*, 1972; Pozas *et al.*, 1975). The square-pyramidal sites form $[Ca_2O_8]$ dimers (Fig. 3d) with the Ca-Ca distance of 3.469 Å. In contrast to calcinaksite, whereas Ca atoms are 6-coordinated, in the investigated sample the Ca atoms are 5-coordinated. The 5-coordinated Ca is exceptionally rare in inorganic compounds (Katz *et al.*, 1996). The Ca atom occupies the center of a distorted square pyramid with five bonds in the range 2.175-2.339 Å (Fig. 3d). In contrast to litidionite or Ti-bearing litidionite with $Cu^{2+}$ cation at the *M* site, in enricofrancoite there is no strong Jahn–Teller distortion observed. There are two relatively short bonds for Ca-O of 2.187 and 2.175 Å and three bonds with more appropriate distances of 2.204, 2.269 and 2.339 Å. The mean bond distance is 2.235 Å. The





https://doi.org/10.1180/mgm.2024.9 Published online by Cambridge University Press

refined occupancy of *M* site $(Ca_{0.71}Mg_{0.19}Cu_{0.10})_{1.00}$ well agrees with its BVS sum of 2.08 *v.u* (Table 7).

The heteropolyhedral framework of enricofrancoite is characterized by a two-dimensional system of crossing channels running along the [110] and near parallel to [010] directions of the triclinic cell. For non-isometric channels with an elliptical cross-section, according to IUPAC nomenclature, the lengths of the major and minor axes subtracting the ionic radii of $O^{2-}$ of 2.7 Å are used (McCusker *et al.*, 2003). Channel I (Fig. 4a), running along [010], is characterized by an octagonal cross-section and an effective diameter equal to 4.31 × 1.26 $Å^2$.

Channel II (Fig. 4b) parallel to [110] direction also has an octagonal cross-section with an effective diameter of 2.88 × 1.87 $Å^2$. Channels I and II overlap and form a two-dimensional system of cavities populated by $K^+$ cations. The K atom is 8-coordinated with the mean <K−O> distance of 2.943 Å.

Channel III is composed by four $SiO_4$ tetrahedra and two $CaO_5$ pyramids. The channel III runs along [110] direction and has a hexagonal cross-section and an effective diameter of 1.61 × 1.16 $Å^2$. This type of channels is filled by $Na^+$ cations. The Na1 site in the enricofrancoite structure is 6-coordinated with a mean <Na-O> distance of 2.555 Å. It should be noted weak character of Na-O3 bond with distance of 2.997 Å, which gives only (0.04 *v.u*) according to the BVS data. According to the BVS data (Table 7), all O sites are fully populated by $O^{2-}$.

The formula refined from SC-XRD data can be written as $KNa(Ca_{0.71}Mg_{0.19}Cu_{0.10})_{1.00}(Si_4O_{10})$.

**Raman and FTIR**

Raman spectra of enricofrancoite were recorded with a Horiba Jobin-Yvon LabRAM HR800 spectrometer equipped with an Olympus BX-41 microscope in backscattering geometry via CCD detector. For the measurements were used uncoated polished sections from the same grain, for which EPMA was made. Raman spectra were recordered by 514 nm Ar laser with power of 2 mW





https://doi.org/10.1180/mgm.2024.9 Published online by Cambridge University Press

under the 50x objective with a numerical aperture equal to 0.75. The spectra were obtained in the range of 40–4000 $cm^{-1}$ at a resolution of 2 $cm^{-1}$ at room temperature with a 150 μm aperture diameter and 240 sec acquisition time. To improve the signal-to-noise ratio, the number of acquisitions was set to 6. For the control of damage of the sample, the photos of sample surface before and after analysis were made. The spectra were processed using Labspec and Origin software. The attribution of observed bands was made according to other minerals of the litidionite group (Balassone *et al.*, 2022).

Fourier Transform Infrared spectroscopy, performed on a powered sample in Attenuated Total Reflectance mode (ATR–FTIR), was used in the spectral range 4000–400 $cm^{-1}$ with resolution 2 $cm^{-1}$ (Bruker Alpha; Opus 7.2 software–Bruker Optik GmbH, Leipzig, Germany).

The Raman spectrum of enricofrancoite (Fig. 5) is similar to those both Vesuvius litidionite sample R130088 of the RRUFF project (Lafuente *et al.*, 2015) and Ti-bearing litidionite (Balassone *et al.*, 2022), but have some differences. The spectrum band (s=strong band, w=weak band, sh=shoulder) at 1120 (s), can be assigned to the symmetric stretching vibrations of the Si-O bands in the $[Si_8O_{20}]^{8-}$ groups (Yakovenchuk *et al.*, 2019; Balassone *et al.*, 2022). Bands at 690 and 600 (s) $cm^{-1}$ related to asymmetric bending vibrations of Si–O–Si and O–Si–O bonds. The bands centred at 510, 438 (w), 400, 335 (w) $cm^{-1}$ are attributed to different modes of bending vibrations in $SiO_4$ tetrahedra (Pakhomovsky *et al.*, 2018). Bands at 248, 265, 290 $cm^{-1}$ can be assigned to symmetric vibrations of Ca–O bonds (Galuskin *et al.*, 2012). The band at 133 (w) $cm^{-1}$ corresponds to the lattice mode vibrations. The absence of bands in the ranges of 1550 to 1650 and 3000-3700 $cm^{-1}$, respectively corresponding to the bending H–O–H and stretching vibrations of bonds in water molecules and OH-groups, is in accordance with undetectable $H_2O$ content in the enricofrancoite composition.

The IR spectrum of enricofrancoite is given in Fig. 6. In general, the IR spectrum of enricofrancoite is somewhat similar to those of the structurally related calcinaksite, fenaksite and manaksite (Chukanov et al., 2015). Wavenumbers of absorption bands can be assigned with Si–O–Si bending and stretching vibrations combined with vibrations of Ca–O bonds in $CaO_5$ polyhedra 424





https://doi.org/10.1180/mgm.2024.9 Published online by Cambridge University Press

(s), 470 (sh), 492 (sh) $cm^{-1}$. The bands at 530, 600, 630 (w), 690, 750 and 788 (w) $cm^{-1}$ can be attributed to the bending vibrations of Si–O bonds in the tubular silicate $[Si_8O_{20}]^{8-}$ anionic radical. The bands at 970 (s), 1040 (w), 1160 (sh) correspond to the Si–O stretching vibrations. Bending and stretching vibrations of $H_2O$ molecules have not been observed in contrast to the calcinaksite, which contains certain bands at 1654, 3170, 3340, 3540 $cm^{-1}$ (Chukanov et al., 2015).

**Discussion**

Silicates with tubular fragments, natural and synthetic, are quite rare. In addition to the litidionite family with hexagonal tubes, minerals with octagonal (frankamenite, canasite, miserite) and quadrangular (narsarsukite) tubes, heterogeneous (charoite) and heteropolyhedral tubular fragments (yuksporite) and such compounds often have pronounced magnetic, luminescent and ion-exchange properties (Rainho *et al.*, 2000; Brandão *et al.*, 2009; Day and Hawthorne, 2020). Enricofrancoite is $H_2O$-free analogue of calcinaksite with 5-coordinated $Ca^{2+}$ at the *M* site (also indicated as Ca1). The dominant components in different litidionite-group minerals are listed in Table 8. The most variable site in litidionite-type structure is the *M*-position, its coordination number can vary from 4+1 (for Cu) and 5 (for $Mn^{2+}$, $Fe^{2+}$, Ti and Ca) to 5+1 (Ca) (Fig. 7a) (Rozhdestvenskaya *et al.*, 2004; Karimova and Burns, 2008; Brandão *et al.*, 2009; Aksenov *et al.*, 2014; Balassone *et al.*, 2022). A similar diversity for basically 5-coordinated site is observed for another silicate from Vesuvius, formed in a similar temperature range (500-800 °C), vesuvianite (Balassone *et al.*, 2011). The five-coordinated site in vesuvianite *Y*1 can be predominately occupied by $Fe^{2+}$, $Fe^{3+}$, $Mn^{2+}$, $Mn^{3+}$ Cu, Mg, Al (Groat et al., 1992; Ohkawa et al., 1992; Armbruster et al., 2002; Panikorovskii et al., 2017a, b, c; d). The unit-cell volume of the litidionite-group minerals depends on the coordination number of the *M*-site (Fig. 7b). The unit-cell volume increases together with the coordination number of the *M*-site. Such variability is the key for the new litidionite-group mineral search and for the synthesis of new compounds with litidionite structure, being Co and Ni analogues already synthetized (Durand *et al.*, 1997).





https://doi.org/10.1180/mgm.2024.9 Published online by Cambridge University Press

The litidionite-crystal-structure type is unique because it may contain Ca with coordination both number 5 and 6, which is extremely rare for inorganic compounds. It seems that the Ca coordination depends on the formation conditions.

During the voting on the new mineral proposal, one comment was related to the possible formation of enricofrancoite through the dehydration calcinaksite, because the sample has been stored in a museum collection for a long time. In favor of this assertion is a small contraction of the volume between enricofrancoite 472.74 and calcinksite 495.94 $Å^3$.

The most unstable minerals in fumarolic environments at normal temperatures water-free are typically associated with halides. For example, sanguite, $KCuCl_3$ in humid air alters to eriochalcite $CuCl_2 \times 2H_2O$ and sylvite KCl after several weeks (Pekov *et al.*, 2015). Another example is saranchinaite, $Na_2Cu(SO_4)_2$, which transforms into kröhnkite, $Na_2Cu(SO_4)_2 \times 2H_2O$, during one week if exposed at ambient conditions (87% humidity and 25°C) (Siidra *et al.*, 2018). At the same time, the dehydration process is also possible; for example, kröhnkite is replaced by saranchinaite if heated to a temperature above 200 °C (Hawthorne and Ferguson, 1975). Silicate minerals are more stable and do not usually change in chemical composition, for example analcime, cancrinite, chabazite-K, gonnardite, phillipsite-K, thomsonite-Ca, scolecite from Somma-Vesuvius Complex don't lose water during storage in a museum.

Theoretically, enricofrancoite can be transformed into calcinaksite by a reaction: $KNaCaSi_4O_{10} + H_2O \rightarrow KNaCaSi_4O_{10} \times H_2O$. Figures 8a,b show the local coordination of *M*-position within Na-containing channels along [110] direction in calcinaksite and enricofrancoite, respectively. The presence of additional $H_2O$ molecule in calcinaksite leads to an increase channels size, for example, the O4-O4 distance increases from 4.31 in enricofrancoite to 5.15 Å in calcinaksite. The change of the coordination number for the *M*-site significantly distorts the framework and affects the geometry of the $Si_8O_{20}$ tubes. The large diagonal (Fig. 8c,d) decreases from 5.69 to 5.16 Å and the small diagonal increases from 3.27 to 3.41 Å in enricofrancoite compared with calcinaksite. Thus, the hydration reaction entails global changes in the mineral structure, which requires significant energy





https://doi.org/10.1180/mgm.2024.9 Published online by Cambridge University Press

and this is unlikely at room conditions. The most possible condition is that such a reaction will be connected with crystallinity loss. Thus, we believe that a spontaneous transition from enricofrancoite to calcinaksite is unlikely, and such a rearrangement of the structure is likely to entail a loss of crystallinity.

## Conclusions

Enricofrancoite with litidionite associations of Somma-Vesuvius are typically found in deep blue glassy crusts and characterize very unusual thermally modified pyroclastic fragments related to the old fumarolic activity of the 1872 eruption (Scacchi, 1880; Pozas *et al.*, 1975). Whereas calcinaksite is a product of contact metamorphism formed during the relatively high temperature hydrothermal stage (estimated temperature of crystallization is 300 °C), the enricofrancoite can be formed in the temperature range 600–800 °C (hydrogen-free), as a result of direct deposition from the gas phase (as volcanic sublimates) or gas–rock interactions. The occurrence of coexisting litidionite-group minerals (earlier litidionite and later 'Ti-litidionite'), which do not contain OH and $H_2O$ in their composition, corroborates this observation. The formation of enricofrancoite as a product of dehydration calcinaksite can be possible, but requires significant structural changes and likely leads to loss of crystallinity.



## Acknowledgements

Authors are grateful to Principal Editor Prof. Stuart Mills and referees Prof. Peter Leverett and two anonymous reviewers for the constructive comments significantly improved paper quality. This research was funded by the Russian Science Foundation, project no. 21-77-10103 (TLP) and by the State Assignment of the Russian Academy of Sciences, theme #FMEZ-2022-0022 (OFG). Funding



https://doi.org/10.1180/mgm.2024.9 Published online by Cambridge University Press

from University of Naples Federico II (Ric. Dip. 2018-2020) granted to G.B. are also acknowledged. Thanks are due to Prof. M. Mercurio (Università del Sannio, Benevento, Italy), for allowing the use of the FTIR instrumentation at the Department of Science and Technology.

## References

Agilent Technologies. (2014) CrysAlis CCD and CrysAlis RED. *Oxford Diffraction Ltd, Yarnton, Oxfordshire*.

Aksenov, S.M., Rastsvetaeva, R.K., Chukanov, N. V. and Kolitsch, U. (2014) Structure of calcinaksite KNa[Ca($H_2O$)][$Si_4O_{10}$], the first hydrous member of the litidionite group of silicates with $[Si_8O_{20}]_8-$ tubes. *Acta Crystallographica Section B Structural Science, Crystal Engineering and Materials*, **70**, 768–775.

Armbruster, T., Gnos, E., Dixon, R., Gutzmer, J., Hejny, C., Döbelin, N. and Medenbach, O. (2002) Manganvesuvianite and tweddillite, two new Mn3+-silicate minerals from the Kalahari manganese fields, South Africa. *Mineralogical Magazine*, **66**, 121–135.

Balassone, G., Talla, D., Beran, A., Mormone, A., Altomare, A., Moliterni, A., Mondillo, N., Saviano, M. and Petti, C. (2011) Vesuvianite from Somma-Vesuvius volcano (southern Italy): Chemical, X-ray diffraction and single-crystal polarized FTIR investigations. *Periodico di Mineralogia*, **80**, 369–384.

Balassone, G., Petti, C., Mondillo, N., Panikorovskii, T.L., de Gennaro, R., Cappelletti, P., Altomare, A., Corriero, N., Cangiano, M. and D'Orazio, L. (2019) Copper Minerals at Vesuvius Volcano (Southern Italy): A Mineralogical Review. *Minerals*, **9**, 730.

Balassone, G., Panikorovskii, T.L., Pellino, A., Bazai, A. V., Bocharov, V.N., Krivovichev, S. V., Petti, C., Cappelletti, P. and Mondillo, N. (2022) The complex mechanism of $Ti^{4+}$ incorporation into litidionite from the Somma–Vesuvius volcano, Italy. *Mineralogical Magazine*, **86**, 222–233.

Balassone, P., Panikorovskii, T.L., Pellino, A., Bazai, A.V., Bocharov, V.N., Goychuk, O.F., Avdontseva, E.Y., Yakovenchuk, V.N., Krivovichev, S.V., Petti, C., Cappelletti, P.A., Mondillo,





https://doi.org/10.1180/mgm.2024.9 Published online by Cambridge University Press

N., Moliterni, A. and Altomare, A. (2023) Enricofrancoite, IMA 2023-002. CNMNC Newsletter 74. *Eur. J. Mineral*, **35**, 659–664.

Baur, W.H. (1974) The geometry of polyhedral distortions. Predictive relationships for the phosphate group. *Acta Crystallographica Section B Structural Crystallography and Crystal Chemistry*, **30**, 1195–1215.

Brandão, P., Rocha, J., Reis, M.S., dos Santos, A.M. and Jin, R. (2009) Magnetic properties of compounds. *Journal of Solid State Chemistry*, **182**, 253–258.

Brese, N.E. and O'Keefe M. (1991) Bond-valence parameters for solids. *Acta Crystallographica*, **B47**, 192-197.

Chukanov, N. V., Aksenov, S.M., Rastsvetaeva, R.K., Blass, G., Varlamov, D.A., Pekov, I. V., Belakovskiy, D.I. and Gurzhiy, V. V. (2015) Calcinaksite, $KNaCa(Si_4O_{10})H2O$, a new mineral from the Eifel volcanic area, Germany. *Mineralogy and Petrology*, **109**, 397–404.

Day, M.C. and Hawthorne, F.C. (2020) A structure hierarchy for silicate minerals: chain, ribbon, and tube silicates. *Mineralogical Magazine*, **84**, 165–244.

Dolivo-Dobrovolsky, D.D. (2016) MINAL, free software. Saint-Petersburg. <http://www.dimadd.ru>.

Dolomanov, O. V., Bourhis, L.J., Gildea, R.J., Howard, J.A.K. and Puschmann, H. (2009) OLEX2: a complete structure solution, refinement and analysis program. *Journal of Applied Crystallography*, **42**, 339–341.

Durand, G., Vilminot, S., Richard-Plouet, M., Derory, A., Lambour, J.P. and Drillon, M. (1997) Magnetic Behavior of $Na_2MSi_4O_{10}$ (M=Co, Ni) Compounds. *Journal of Solid State Chemistry*, **131**, 335–340.

Franco, E. and de Gennaro, M. (1988) Panunzite; a new mineral from Mt. Somma-Vesuvio, Italy. *American Mineralogist*, **73**, 420–421.

Galuskin, E. V., Lazic, B., Armbruster, T., Galuskina, I.O., Pertsev, N.N., Gazeev, V.M., Wlodyka, R., Dulski, M., Dzierzanowski, P., Zadov, A.E. and Dubrovinsky, L.S. (2012) Edgrewite





https://doi.org/10.1180/mgm.2024.9 Published online by Cambridge University Press

$Ca_9(SiO_4)_4F_2$-hydroxyledgrewite $Ca_9(SiO_4)_4(OH)_2$, a new series of calcium humite-group minerals from altered xenoliths in the ignimbrite of Upper Chegem caldera, Northern Caucasus, Kabardino-Balkaria, Russia. *American Mineralogist*, **97**, 1998–2006.

de Gennaro, M. and Franco, E. (1974) La K-Cabasite di alcuni «tufi del Vesuvio». *Atti della Accademia Nazionale dei Lincei*, **60**, 490–497.

Golovachev, V.P., Drozdov, Y.N., Kuz'min, E.A. and Belov, N.V. (1970) The crystal structure of fenaksite, $NaKFeSi_4O_{10}$. *Doklady Akademii Nauk SSSR*, **194**, 818-820 (in Russian).

Groat, L.A., Hawthorne, F.C. and Ercit, T.S. (1992) The chemistry of Vesuvianite. *The Canadian Mineralogist*, **30**, 19–48.

Hawthorne, F.C. and Ferguson, R.B. (1975) Refinement of the crystal structure of kröhnkite. *Acta Crystallographica Section B Structural Crystallography and Crystal Chemistry*, **31**, 1753–1755.

Holland, T.J.B. and Redfern, S.A.T. (1997) Unit cell refinement from powder diffraction data: the use of regression diagnostics. *Mineralogical Magazine*, **61**, 65–77.

Karimova, O. and Burns, P.C. (2008) Silicate Tubes in the Crystal Structure of Manaksite. Pp. 153–156 in: *Minerals as Advanced Materials I*. Springer Berlin Heidelberg, Berlin, Heidelberg.

Katz, A.K., Glusker, J.P., Beebe, S.A. and Bock, C.W. (1996) Calcium Ion Coordination: A Comparison with That of Beryllium, Magnesium, and Zinc. *Journal of the American Chemical Society*, **118**, 5752–5763.

Khomyakov, A.P., Kurova, T.A. and Nechelyustov, G.N. (1992) Manaksite $NaKMnSi_4O_{10}$: a new mineral. *Zapiski RMO*, **121**, 112–114.

Kornev, A.N., Maksimov, B.A., Lider, V.V., Ilyukhin, V.V. and Belov, N.V. (1972) Crystal structure of Na2CuSi4O10. *Soviet Physics Doklady*, **17**, 735–737.

Lafuente, B., Downs, R.T., Yang, H. and Stone, N. (2015) The power of databases: the RRUFF project. Pp. 1–30 in: *Highlights in Mineralogical Crystallography*.

Liebau, F. (1985) *Structural Chemistry of Silicates*. P. in.: Springer Berlin Heidelberg, Berlin, Heidelberg.





https://doi.org/10.1180/mgm.2024.9 Published online by Cambridge University Press

McCusker, L.B., Liebau, F. and Engelhardt, G. (2003) Nomenclature of structural and compositional characteristics of ordered microporous and mesoporous materials with inorganic hosts. *Microporous and Mesoporous Materials*, **58**, 3–13.

Merlino, S., Franco, E., Mattia, C.A., Pasero, M. and De Gennaro, M. (1985) The crystal structure of panunzite (natural tetrakalsilite). *Neues Jahrbuch Fur Mineralogie Monatshefte*, **7**, 322–328.

Momma, K. and Izumi, F. (2011) VESTA 3 for three-dimensional visualization of crystal, volumetric and morphology data. *Journal of Applied Crystallography*, **44**, 1272–1276.

Ohkawa, M., Yoshiasa, A. and Takeno, S. (1992) Crystal chemistry of vesuvianite: site preferences of square- pyramidal coordinated sites. *American Mineralogist*, **77**, 945–953.

Pakhomovsky, Y.A., Panikorovskii, T.L., Yakovenchuk, V.N., Ivanyuk, G.Yu., Mikhailova, J.A., Krivovichev, S. V., Bocharov, V.N. and Kalashnikov, A.O. (2018) Selivanovaite, $NaTi_3(Ti,Na,Fe,Mn)_4[(Si_2O_7)_2O_4(OH,H_2O)_4]\cdot nH_2O$, a new rock-forming mineral from the eudialyte-rich malignite of the Lovozero alkaline massif (Kola Peninsula, Russia). *European Journal of Mineralogy*, **30**, 525–535.

Panikorovskii, T.L., Chukanov, N.V., Aksenov, S.M., Mazur, A.S., Avdontseva, E.Yu., Shilovskikh, V.V. and Krivovichev, S.V. (2017a) Alumovesuvianite, Ca19Al(Al,Mg)12Si18O69(OH)9, a new vesuvianite-group member from the Jeffrey mine, asbestos, Estrie region, Québec, Canada. *Mineralogy and Petrology*, **111**, 833–842. Mineralogy and Petrology.

Panikorovskii, T.L., Shilovskikh, V.V., Avdontseva, E.Yu., Zolotarev, A.A., Pekov, I.V., Britvin, S.N., Hålenius, U. and Krivovichev, S.V. (2017b) Cyprine, $Ca_{19}Cu^{2+}(Al,Mg,Mn)_{12}Si_{18}O_{69}(OH)_9$, a new vesuvianite-group mineral from the Wessels mine, South Africa. *European Journal of Mineralogy*, **29**, 295–306.

Panikorovskii, T.L., Shilovskikh, V.V., Avdontseva, E.Yu., Zolotarev, A.A., Karpenko, V.Yu., Mazur, A.S., Yakovenchuk, V.N., Bazai, A.V., Krivovichev, S.V. and Pekov, I.V. (2017c) Magnesiovesuvianite, $Ca_{19}Mg(Al,Mg)_{12}Si_{18}O_{69}(OH)_9$, a new vesuvianite-group mineral. *Journal of Geosciences (Czech Republic)*, **62**, 25–36.





https://doi.org/10.1180/mgm.2024.9 Published online by Cambridge University Press

Panikorovskii, T.L., Chukanov, N.V., Rusakov, V.S., Shilovskikh, V.V., Mazur, A.S., Balassone, G., Ivanyuk, G.Yu. and Krivovichev, S.V. (2017d) Vesuvianite from the Somma-Vesuvius Complex: New Data and Revised Formula. *Minerals*, **7**, 248.

Pekov, I. V., Zubkova, N. V., Belakovskiy, D.I., Lykova, I.S., Yapaskurt, V.O., Vigasina, M.F., Sidorov, E.G. and Pushcharovsky, D.Yu. (2015) Sanguite, $KCuCl_3$ , A New Mineral From the Tolbachik Volcano, Kamchatka, Russia. *The Canadian Mineralogist*, **53**, 633–641.

Pozas, J.M., Rossi, G. and Tazzoli, V. (1975) Re-examination and Crystal Structure Analysis of Litidionite. *American Mineralogist*, **60**, 471–474.

Rainho, J.P., Carlos, L.D. and Rocha, J. (2000) New phosphors based on Eu3+-doped microporous titanosilicates. *Journal of Luminescence*, **87–89**, 1083–1086.

Rozhdestvenskaya, I.V., Bannova, I.I., Nikishova, L.V. and Soboleva, T.V. (2004) The crystal structure of fenaksite $K_2Na_2Fe_2Si_8O_{20}$. *Doklady of the Russian Academy of Sciences*, **398**, 1029–1033.

Scacchi, E. (1880) Lapilli azzurri del Vesuvio. *Rendiconto dell'Accademia delle Scienze Fisiche e Matematiche*, **19**, 175–179.

Sheldrick, G.M. (2015) Crystal structure refinement with SHELXL. *Acta Crystallographica Section C Structural Chemistry*, **71**, 3–8.

Siidra, O.I., Lukina, E.A., Nazarchuk, E. V., Depmeier, W., Bubnova, R.S., Agakhanov, A.A., Avdontseva, E.Yu., Filatov, S.K. and Kovrugin, V.M. (2018) Saranchinaite, $Na_2Cu(SO_4)_2$ , a new exhalative mineral from Tolbachik volcano, Kamchatka, Russia, and a product of the reversible dehydration of kröhnkite, $Na_2Cu(SO_4)_2(H_2O)_2$. *Mineralogical Magazine*, **82**, 257–274.

Yakovenchuk, V., Pakhomovsky, Y., Panikorovskii, T., Zolotarev, A., Mikhailova, J., Bocharov, V., Krivovichev, S. and Ivanyuk, G. (2019) Chirvinskyite, $(Na,Ca)_{13}(Fe,Mn,□)_2(Ti,Nb)_2(Zr,Ti)^{3-}(Si_2O_7)_4(OH,O,F)_{12}$, a New Mineral with a Modular Wallpaper Structure, from the Khibiny Alkaline Massif (Kola Peninsula, Russia). *Minerals*, **9**, 219.





https://doi.org/10.1180/mgm.2024.9 Published online by Cambridge University Press

**Table 1.** Chemical data (in wt. %) for enricofrancoite.

| wt.% | 1 | 2 | 3 | Reference material |
|---|---|---|---|---|
| $SiO_2$ | 66.35 | 64.15 | 63.92 | Wollastonite |
| $Al_2O_3$ | 0.02 | 0.05 | 0.03 | Pyrope |
| $TiO_2$ | 0.08 | 0.12 | 0.04 | Lorenzenite |
| FeO | 0.08 | 0.09 | 0.05 | Hematite |
| MgO | 1.52 | 1.55 | 2.06 | Pyrope |
| CaO | 11.37 | 10.62 | 9.94 | Wollastonite |
| CuO | 2.07 | 1.60 | 3.00 | Copper |
| $Na_2O$ | 8.98 | 8.52 | 8.17 | Lorenzenite |
| $K_2O$ | 10.35 | 11.82 | 12.06 | Wadeite |
| Total | 100.82 | 98.53 | 99.28 | |
| calculated on the basis of O=10 *apfu* | | | | |
| $Si^{4+}$ | 4.04 | 4.03 | 4.00 | |
| $Al^{3+}$ | - | - | - | |
| $Ti^{4+}$ | - | 0.01 | - | |
| $Fe^{2+}$ | - | - | - | |
| $Mg^{2+}$ | 0.14 | 0.14 | 0.19 | |
| $Ca^{2+}$ | 0.74 | 0.71 | 0.67 | |
| $Cu^{2+}$ | 0.10 | 0.08 | 0.14 | |
| $Na^{+}$ | 1.06 | 1.04 | 0.99 | |
| $K^{+}$ | 0.80 | 0.95 | 0.96 | |





https://doi.org/10.1180/mgm.2024.9 Published online by Cambridge University Press

**Table 2.** Crystal data, data collection information and structure refinement details for enricofrancoite.

| | |
|---|---|
| Temperature/K | 293(2) |
| Crystal system | Triclinic |
| Space group | *P*-1 |
| *a*/Å | 7.0155(4) |
| *b*/Å | 8.0721(4) |
| *c*/Å | 10.0275(4) |
| *α*/° | 104.420(4) |
| *β*/° | 99.764(4) |
| *γ*/° | 115.126(5) |
| Volume/Å$^3$ | 472.74(5) |
| *Z* | 2 |
| $\rho_{calc}$ g/cm$^3$ | 2.627 |
| $\mu$/mm$^{-1}$ | 1.775 |
| F(000) | 371.0 |
| Crystal size/mm$^3$ | 0.12 × 0.11 × 0.05 |
| Radiation | Mo *K*α (λ = 0.71073) |
| 2Θ range for data collection/° | 5.974 to 58.616 (full completness for 50.5° and 80% for 58.6°) |
| Index ranges | -8 ≤ h ≤ 9, -10 ≤ k ≤ 10, -13 ≤ l ≤ 12 |
| Reflections collected | 4065 |
| Independent reflections | 2078 [$R_{int}$ = 0.0146, $R_{sigma}$ = 0.0263] |
| Data/restraints/parameters | 2078/0/154 |
| Goodness-of-fit on $F^2$ | 1.125 |
| Final *R* indexes [$I$>2σ ($I$)] | $R_1$ = 0.0348, w$R_2$ = 0.0826* |
| Final *R* indexes [all data] | $R_1$ = 0.0395, w$R_2$ = 0.0854 |
| Largest diff. peak/hole / e Å$^{-3}$ | 0.73/-0.53 |
| *Weighting scheme 0.0299 | 1.0128 |





https://doi.org/10.1180/mgm.2024.9 Published online by Cambridge University Press

**Table 3.** Fractional atom coordinates, site occupancies (s.o.) and equivalent isotropic atomic displacement parameters $U_{eq}$ (Å$^2$) for enricofrancoite.

| Atom | s.o. | *x* | *y* | *z* | $U_{eq}$ |
|---|---|---|---|---|---|
| Ca1 (= *M*) | $Ca_{0.71}Mg_{0.19}Cu_{0.10}$ | 0.33953(10) | 0.88224(9) | 0.09591(7) | 0.0170(2) |
| K1 | $K_{1.00}$ | -0.14661(13) | 0.20386(11) | 0.50851(9) | 0.0304(2) |
| Si1 | $Si_{1.00}$ | 0.08059(14) | 0.37154(13) | 0.22533(11) | 0.0231(2) |
| Si2 | $Si_{1.00}$ | 0.55298(13) | 0.71354(12) | 0.29204(9) | 0.0140(2) |
| Si3 | $Si_{1.00}$ | 0.30959(15) | 1.18447(13) | 0.36887(9) | 0.0193(2) |
| Si4 | $Si_{1.00}$ | 0.35139(14) | 0.62847(13) | -0.23022(11) | 0.0216(2) |
| Na1 | $Na_{1.00}$ | 0.8427(2) | 0.8717(2) | 0.09196(14) | 0.0262(3) |
| O1 | $O_{1.00}$ | -0.0912(4) | 0.4316(4) | 0.2871(3) | 0.0324(6) |
| O2 | $O_{1.00}$ | 0.1948(4) | 0.9661(4) | 0.2620(3) | 0.0325(6) |
| O3 | $O_{1.00}$ | 0.3501(5) | 0.4270(4) | -0.2276(4) | 0.0424(8) |
| O4 | $O_{1.00}$ | 0.1633(4) | 1.2902(4) | 0.3436(3) | 0.0345(6) |
| O5 | $O_{1.00}$ | 0.3429(7) | 1.1972(5) | 0.5346(3) | 0.0625(9) |
| O6 | $O_{1.00}$ | 0.6175(4) | 0.8887(4) | 0.2362(3) | 0.0264(5) |
| O7 | $O_{1.00}$ | 0.2880(4) | 0.5814(4) | 0.2480(4) | 0.0504(9) |
| O8 | $O_{1.00}$ | 0.5544(4) | 1.3185(4) | 0.3606(3) | 0.0296(6) |
| O9 | $O_{1.00}$ | 0.4848(4) | 0.8067(3) | -0.0807(3) | 0.0251(5) |
| O10 | $O_{1.00}$ | -0.0244(4) | 0.2188(4) | 0.0661(3) | 0.0312(6) |





https://doi.org/10.1180/mgm.2024.9 Published online by Cambridge University Press

**Table 4.** Anisotropic atomic displacement parameters (Å$^2$) for enricofrancoite.

| Atom | $U^{11}$ | $U^{22}$ | $U^{33}$ | $U^{23}$ | $U^{13}$ | $U^{12}$ |
|---|---|---|---|---|---|---|
| Ca1 | 0.0128(3) | 0.0206(3) | 0.0161(3) | 0.0054(2) | 0.0033(2) | 0.0101(2) |
| K1 | 0.0298(4) | 0.0201(4) | 0.0333(4) | 0.0054(3) | 0.0078(3) | 0.0086(3) |
| Si1 | 0.0122(4) | 0.0166(4) | 0.0372(5) | 0.0028(4) | 0.0090(4) | 0.0076(3) |
| Si3 | 0.0139(4) | 0.0127(4) | 0.0168(4) | 0.0071(3) | 0.0063(3) | 0.0064(3) |
| Si2 | 0.0221(5) | 0.0166(4) | 0.0156(4) | 0.0060(3) | 0.0027(3) | 0.0075(3) |
| Si4 | 0.0103(4) | 0.0142(4) | 0.0346(5) | 0.0012(4) | 0.0044(4) | 0.0062(3) |
| Na1 | 0.0255(7) | 0.0344(8) | 0.0225(7) | 0.0086(6) | 0.0118(5) | 0.0174(6) |
| O1 | 0.0108(11) | 0.0292(14) | 0.0388(14) | -0.0109(11) | 0.0002(10) | 0.0095(10) |
| O2 | 0.0387(15) | 0.0181(12) | 0.0256(13) | 0.0036(10) | -0.0035(11) | 0.0083(11) |
| O3 | 0.0364(15) | 0.0233(14) | 0.086(2) | 0.0234(14) | 0.0390(16) | 0.0210(12) |
| O4 | 0.0285(14) | 0.0381(15) | 0.0410(15) | 0.0096(12) | 0.0112(12) | 0.0224(12) |
| O5 | 0.104(3) | 0.0303(16) | 0.0172(13) | 0.0097(12) | 0.0026(15) | 0.0080(17) |
| O6 | 0.0382(14) | 0.0220(12) | 0.0268(12) | 0.0154(10) | 0.0168(11) | 0.0156(11) |
| O7 | 0.0138(12) | 0.0277(15) | 0.104(3) | 0.0216(16) | 0.0118(15) | 0.0087(11) |
| O8 | 0.0177(12) | 0.0280(13) | 0.0321(13) | 0.0019(11) | 0.0046(10) | 0.0081(10) |
| O9 | 0.0170(11) | 0.0226(12) | 0.0278(12) | 0.0043(10) | 0.0004(9) | 0.0081(10) |
| O10 | 0.0337(14) | 0.0332(14) | 0.0321(13) | 0.0079(11) | 0.0183(11) | 0.0202(12) |





https://doi.org/10.1180/mgm.2024.9 Published online by Cambridge University Press

**Table 5.** Selected interatomic distances (Å) for the crystal structure of enricofrancoite.

| | | | | | |
|---|---|---|---|---|---|
| Ca1 – O9 | 2.339(3) | Si3 – O5 | 1.609(3) | K1 – O2 | 2.955(3) |
| Ca1 – O9 | 2.269(2) | <Si3–O> | 1.605 | K1 – O8 | 2.955(3) |
| Ca1 – O6 | 2.175(3) | | | K1 – O4 | 2.907(3) |
| Ca1 – O2 | 2.204(3) | Si4 – O9 | 1.581(2) | K1 – O1 | 3.190(3) |
| Ca1 – O10 | 2.186(3) | Si4 – O8 | 1.631(3) | K1 – O1 | 2.704(2) |
| <Ca1 – O> | 2.235 | Si4 – O1 | 1.628(2) | K1 – O7 | 3.182(4) |
| | | Si4 – O3 | 1.629(3) | K1 – O5 | 2.807(3) |
| Si2 – O6 | 1.567(2) | <Si4–O> | 1.617 | <K1–O> | 2.943 |
| Si2 – O3 | 1.615(3) | | | | |
| Si2 – O7 | 1.610(3) | Si1 – O10 | 1.569(3) | Na1 – O9 | 2.556(3) |
| Si2 – O5 | 1.604(3) | Si1 – O4 | 1.629(3) | Na1 – O6 | 2.338(3) |
| <Si2–O> | 1.599 | Si1 – O1 | 1.634(2) | Na1 – O2 | 2.433(3) |
| | | Si1 – O7 | 1.625(3) | Na1 – O10 | 2.648(3) |
| Si3 – O2 | 1.570(2) | <Si1–O> | 1.614 | Na1 – O10 | 2.360(3) |
| Si3 – O8 | 1.625(3) | | | Na1 – O3 | 2.997(3) |
| Si3 – O4 | 1.615(3) | K1 – O6 | 2.846(3) | <Na1–O> | 2.555 |

Note: Ca1 = *M*-site





https://doi.org/10.1180/mgm.2024.9 Published online by Cambridge University Press

**Table 6.** PXRD data for enricofrancoite. The intensities, measured $I_{meas}$ (from PXRD data) and calculated $I_{calc}$ (from single-crystal X-ray data), are given with the corresponding interplanar distance values ($d_{meas}$ and $d_{calc}$) and Miller indices (*hkl*). The eight strongest lines are highlighted in bold.

| $I_{meas}$ | $I_{calc}$ | $d_{meas}$, | $d_{calc}$, Å | *hkl* |
|---|---|---|---|---|
| **42** | **70** | **6.75** | **6.75** | **0 1 -1** |
| 16 | 32 | 4.48 | 4.47 | 1 0 1 |
| 17 | 6 | 4.04 | 4.03 | 1 1 -1 |
| **20** | **11** | **3.65** | **3.65** | **1 1 -2** |
| **100** | **100** | **3.370** | **3.375** | **0 2 -2** |
| **52** | **38** | **3.210** | **3.209** | **1 0 2** |
| **18** | **22** | **3.051** | **3.063** | **1 1 1** |
| **25** | **85** | **3.033** | **3.035** | **2 -1 -2** |
| 7 | 6 | 2.980 | 2.986 | 2 -2 -1 |
| **22** | **34** | **2.834** | **2.832** | **0 2 -3** |
| 3 | 3 | 2.674 | 2.675 | 1 2 -2 |
| 11 | 12 | 2.566 | 2.565 | 2 -1 2 |
| 4 | 2 | 2.463 | 2.462 | 1 1 2 |
| **72** | **66** | **2.411** | **2.411** | **0 3 -2** |
| 17 | 20 | 1.9760 | 1.9799 | 2 2 -1 |
| 2 | 2 | 1.9240 | 1.9245 | 3 -3 2 |
| 4 | 4 | 1.9130 | 1.9120 | 3 -3 -2 |
| 3 | 2 | 1.8200 | 1.8182 | 2 -3 4 |
| 3 | 4 | 1.7850 | 1.7870 | 0 4 -3 |





https://doi.org/10.1180/mgm.2024.9 Published online by Cambridge University Press

**Table 7.** Bond-valence analysis (in valence units, v.u.) in the crystal structure of enricofrancoite calculated using bond valence parameters from (Brese and O'Keeffe, 1991).

| atom | Ca1* | Si1 | Si2 | Si3 | Si4 | K1 | Na1 | ∑ |
|---|---|---|---|---|---|---|---|---|
| | | | | | | 0.06 | | |
| O1 | | 0.97 | | | 0.99 | 0.21 | | 2.23 |
| O2 | 0.45 | | | 1.16 | | 0.11 | 0.18 | 1.90 |
| O3 | | | 1.02 | | 0.99 | | 0.04 | 2.05 |
| O4 | | 0.99 | | 1.02 | | 0.12 | | 2.13 |
| O5 | | | 1.06 | 1.04 | | 0.16 | | 2.26 |
| O6 | 0.48 | | 1.17 | | | 0.14 | 0.23 | 2.02 |
| O7 | | 1.00 | 1.04 | | | 0.06 | | 2.09 |
| O8 | | | | 1.00 | 0.98 | 0.11 | | 2.09 |
| | 0.31 | | | | | | | |
| O9 | 0.37 | | | | 1.12 | | 0.13 | 1.93 |
| | | | | | | | 0.10 | |
| O10 | 0.47 | 1.16 | | | | | 0.22 | 1.85 |
| ∑ | 2.08 | 4.12 | 4.29 | 4.22 | 4.08 | 0.97 | 0.90 | |

*The BVS sum for *M* site calculated based on the occupancy $[Ca_{0.71}Mg_{0.19}Cu_{0.10}]_{1.00}$.





https://doi.org/10.1180/mgm.2024.9 Published online by Cambridge University Press

**Table 8.** Dominant components at the crystallographic sites for selected litidionite-group minerals.

| Mineral | Na1 | K1 | *M* | Ow (O11)* | Reference |
|---|---|---|---|---|---|
| litidionite | Na | K | $Cu^{2+}$ | □ | Pozas et al. (1975) |
| fenaksite | Na | K | $Fe^{2+}$ | □ | Golovachev et al. (1970) |
| manaksite | Na | K | $Mn^{2+}$ | □ | Khomyakov et al. (1992) |
| calcinaksite | Na | K | Ca | $H_2O$ | Chukanov et al. (2015) |
| enricofrancoite | Na | K | Ca | □ | This work |

*The Ow (O11) coordinates Ca1 (=*M*) site and observed only in the crystal structure of calcinaksite in which Ca is in octahedral coordination (5+1).





https://doi.org/10.1180/mgm.2024.9 Published online by Cambridge University Press


**Fig. 1.** The enricofrancoite-bearing sample (holotype #17926 E6457) from the Royal Mineralogical Museum of Naples University Federico II (modified after Balassone et al., 2022). The length of the Museum label is 7 cm.





https://doi.org/10.1180/mgm.2024.9 Published online by Cambridge University Press

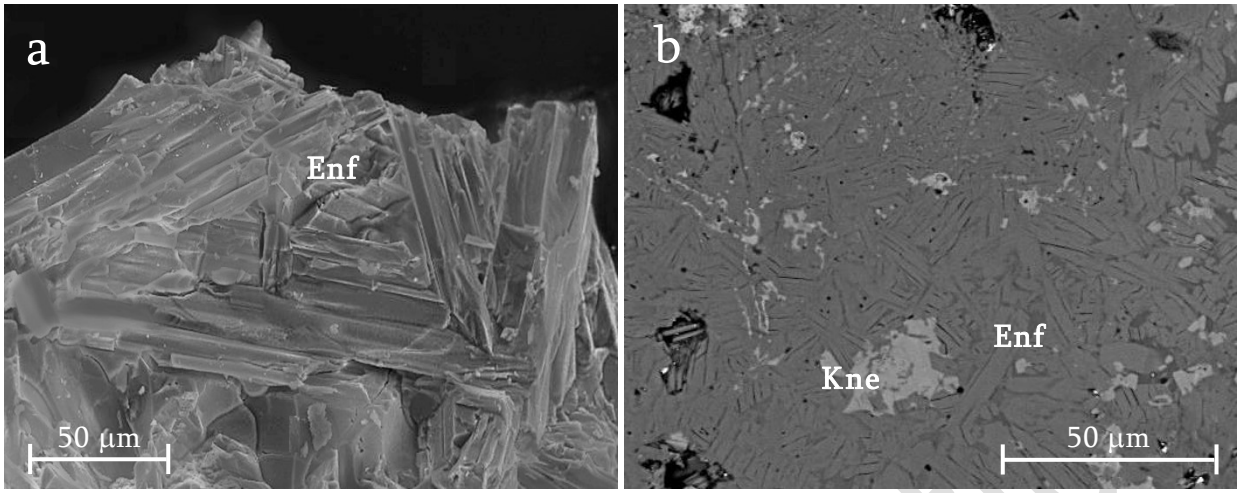


**Fig. 2.** SEM micrograph of enricofrancoite (Enf) in aggregations of platy crystals (holotype #17926 E6457) (a). Enricofrancoite with kamenevite (Kne) in polished thin section, observed in BSE mode (b).





https://doi.org/10.1180/mgm.2024.9 Published online by Cambridge University Press

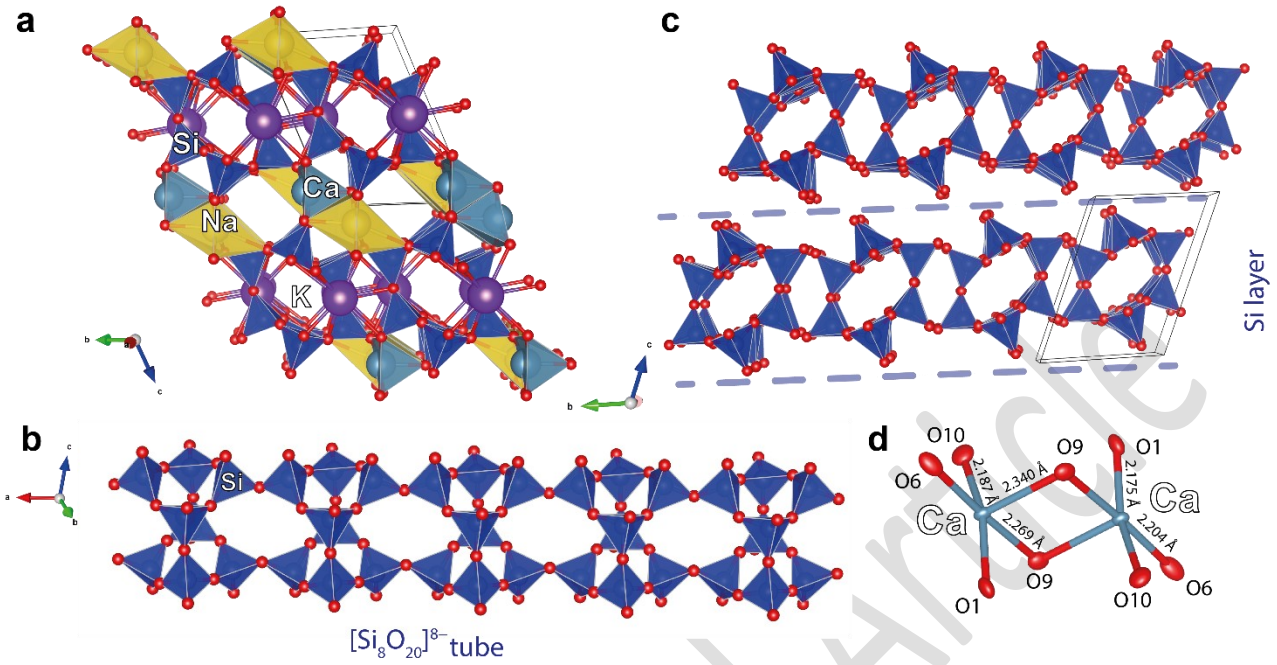


**Fig. 3.** Crystal structure of enricofrancoite: general view (a), silicate tubes (b) silicate layers (c), local coordination of Ca1 site (= *M*) site (d).





https://doi.org/10.1180/mgm.2024.9 Published online by Cambridge University Press

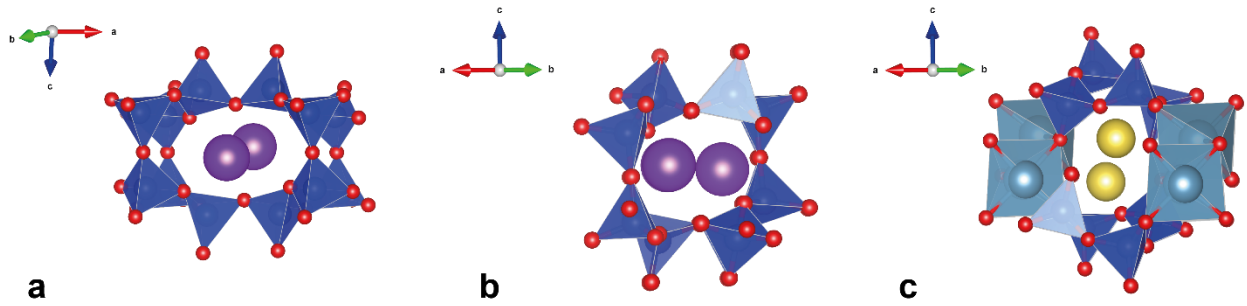


**Fig. 4.** Projections of the channels in the crystal structure of enricofrancoite: along [010] direction (a), two channels along [110] direction(b) and (c).





https://doi.org/10.1180/mgm.2024.9 Published online by Cambridge University Press

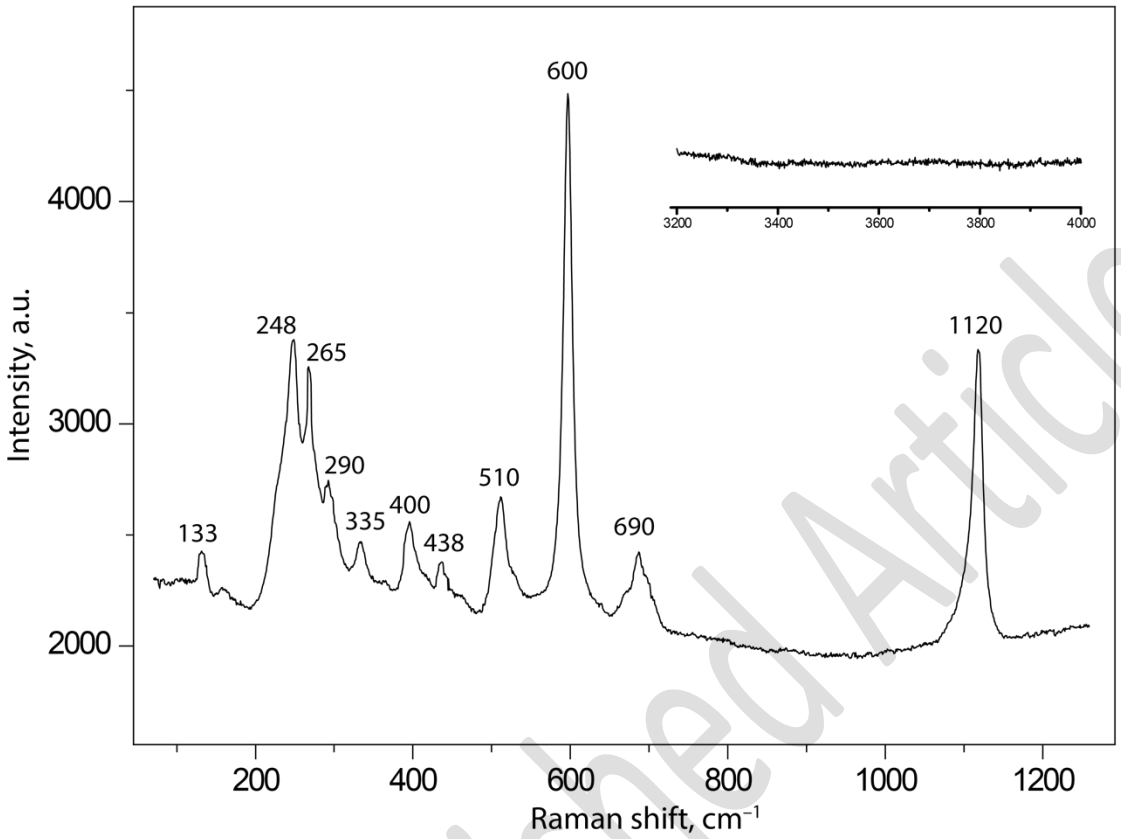


**Fig. 5.** Raman spectrum of enricofrancoite.





https://doi.org/10.1180/mgm.2024.9 Published online by Cambridge University Press

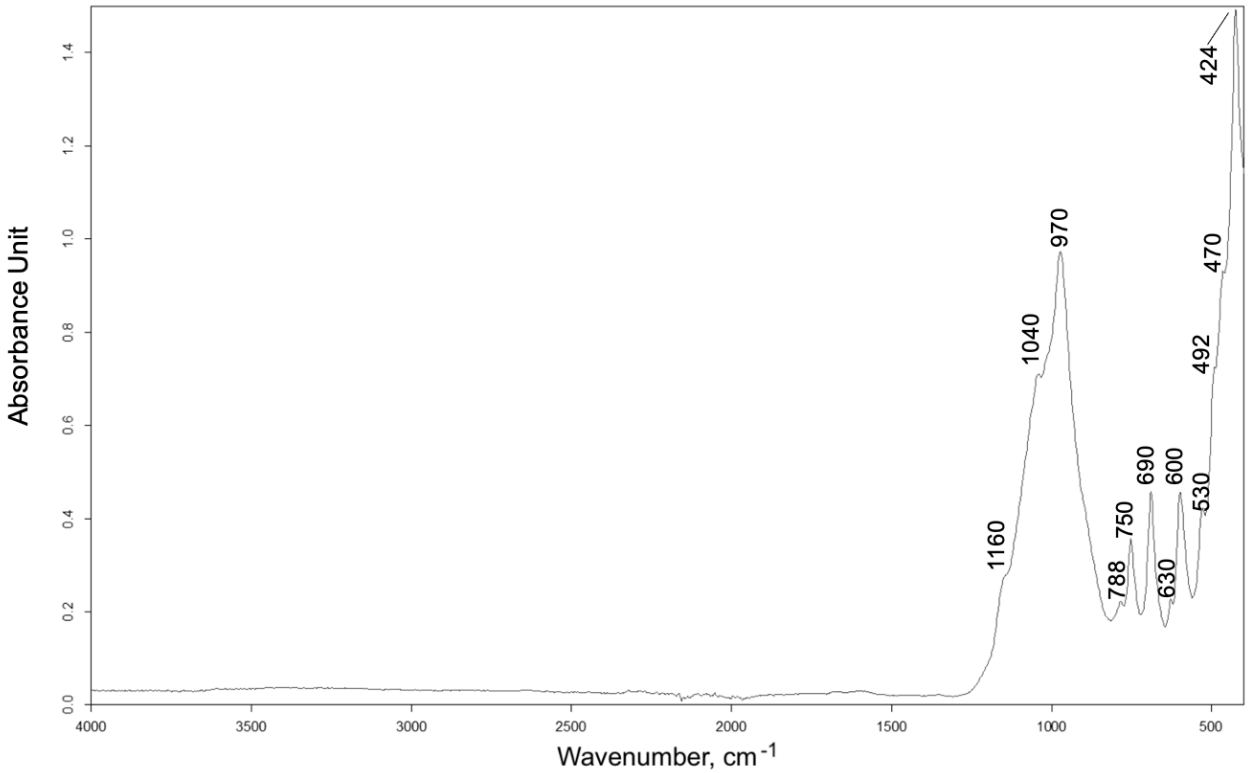


**Fig. 6.** FTIR spectrum of enricofrancoite.





https://doi.org/10.1180/mgm.2024.9 Published online by Cambridge University Press

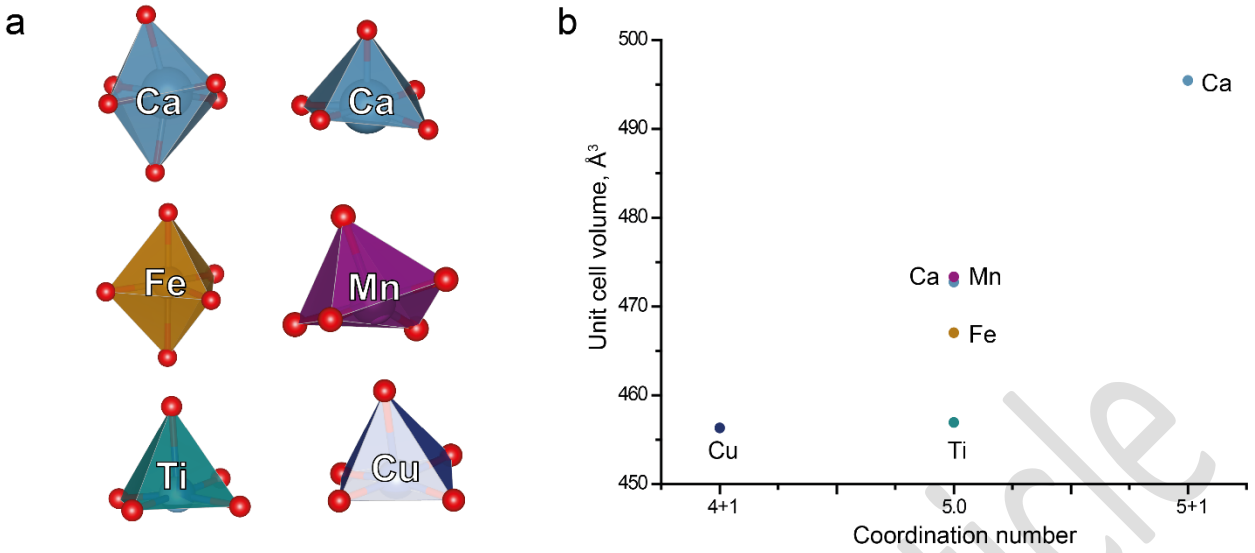


**Fig. 7.** Coordination polyhedra in the minerals of litidionite group based on the data of Rozhdestvenskaya et al. (2004), Karimova and Burns (2008), Brandão et al. (2009), Chukanov et al., 2015) and Balassone et al. (2022). (a); graph of the dependence of unit cell volume on coordination number for litidionitie-group minerals (b).





https://doi.org/10.1180/mgm.2024.9 Published online by Cambridge University Press

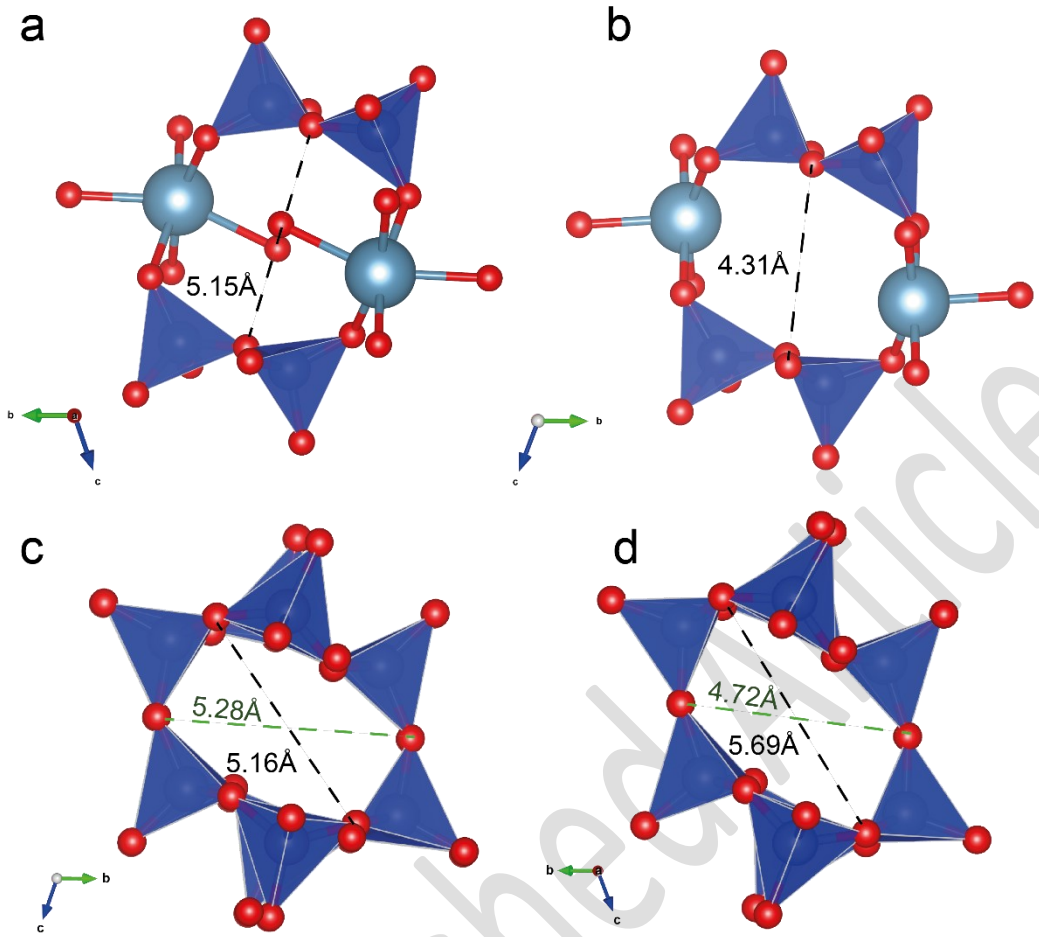


**Fig. 8.** Local coordination of Na-contained channel along [110] direction in the crystal structure of calcinaksite (a) and enricofrancoite (b); geometry of $[Si_8O_{20}]^{8-}$ tubes in the crystal structure of calcinaksite (c) and enricofrancoite (d).





https://doi.org/10.1180/mgm.2024.9 Published online by Cambridge University Press